Icarus 139, 93–99 (1999)
Article ID icar.1999.6089, available online at http://www.idealibrary.com on IDEAL®

Correlation of Venus Surface Features and Geoid

Donna M. Jurdy and Michael Stefanick

Department of Geological Sciences, Northwestern University, Evanston, Illinois 60208-2150
E-mail: donna@earth.nwu.edu

Received April 3, 1998; revised February 1, 1999

The distributions of pairs of features on Venus are compared using simple statistical tests. We consider coronae types, crater types, and chasmata; some of these are obviously associated, and some are possibly associated. Coronae are grouped to represent evolutionary stages, tectonic and volcanic modification of craters is considered, and the chasmata are represented by five great circle arcs. These arcs fit rift or extension zones at the 90% level, totaling 55,000 km, comparable to the length of spreading ridges on Earth. Comparing these sets with Venus' geoid field, we find that all the chasmata correlate positively with geoid highs and negatively with lows, with the peaks in the geoid field occurring at the intersections of the arcs. Modified craters also exhibit this relation to the geoid. The domal coronae, the youngest and currently active, may be sites of upwelling. These correlate strongly with geoid highs and negatively with geoid lows, whereas later-stage coronae, the majority, do not show this correlation. Strong association of the youngest coronae with Themis–Atla suggests that the most recent activity occurs along this arc. © 1999 Academic Press

Key Words: Venus; coronae; geoid; chasmata.

INTRODUCTION

Numerous features adorn the surface of Venus, some impact-related, some volcanic or tectonic in origin, others of unknown genesis. Each feature type has its own nonuniform distribution, and pairs of features seem to either associate with or avoid each other. For example, Stefanick and Jurdy (1996) note coronae concentrations near chasmata; Crumpler *et al.* (1997) point out that volcanic centers are associated with rifting; Phillips *et al.* (1992) and Herrick and Phillips (1994) both observe that modified craters preferentially occur near rift systems, containing both coronae and volcanism. In this paper, we quantitatively compare the distributions of coronae, craters, and the chasmata to ascertain the degree of correlation. The coronae can be described in several ways; here we use the classification of DeLaughter and Jurdy (1999), with groups representing evolutionary stages. The full set of craters is examined, along with subsets modified by tectonism or volcanism. In addition, the location of chasmata and areas of rifting on Venus are considered as is their representation by five great circle arcs. In this paper we go beyond a description of the distribution of features to a statistical comparison of their association or avoidances, using 2×2 contingency tables and ratio tests, which can be related to a χ^2 test. This gives a measure of the degree of association or avoidance of a pair of features, and a quantitative assessment of the correlation and its significance.

The geoid field of Venus and its relation to tectonic features has potential significance. Coronae may be analogs of Earth's hotspots, which strongly correlate with Earth's geoid highs. Therefore, the distributions of the various groups of coronae corresponding to evolutionary stage are compared with the geoid highs; similarly, craters and chasmata, as well as their subsets, are analyzed. If correlations with geoid highs differ according to coronae stage or the geographical location of chasmata, this would suggest a sequential organization of tectonic and volcanic activity.

In the first section we discuss the data sets used (the details of the classification of coronae by evolutionary stage, craters and modified subsets, and the chasmata) and their breakdown and representation by five great circle arcs. Then we outline the method for comparison of discrete objects or fields on a sphere. Next, we present the results for comparison of specific pairs, coronae and craters (including subsets that have been tectonized or embayed); in addition, comparison is made with all chasmata, as well as with individual segments. Last, these features are compared with the geoid field of Venus. A possible chronology is inferred from these correlations.

DATA SETS

For our analysis of surface features on Venus we use coronae, craters (including subsets of these), as well as chasmata and the geoid field. Coronae, common, nearly circular features ranging in size from 100–2600 km in diameter, may be caused by upwelling (Stofan *et al.* 1992) and modify craters out to 4 coronae radii (DeLaughter and Jurdy 1997). For our study we use the set of 331 coronae classified by DeLaughter and Jurdy (1999) in their analysis of 394 features (358 from Stofan *et al.* (1992), 27 from USGS-Flagstaff (1996), 9 from Magee Roberts and Head (1993)). Based on altimetry, they are divided into three groups, although the actual shapes observed are gradational between these. The 50 domal coronae, distinguished by a central uplift

0019-1035/99 $30.00

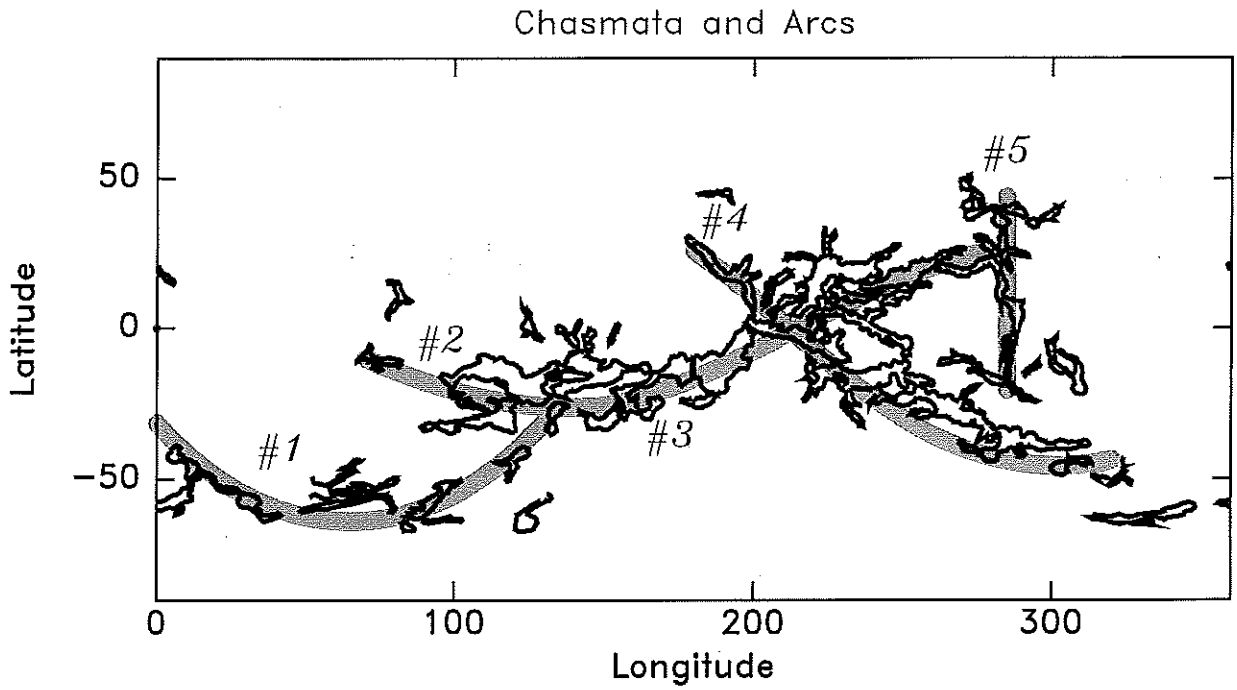

FIG. 1. Rifts as defined by Price and Suppe (1994) are shown, with five numbered great circle arcs that fit these observed extension zones.

with no surrounding moat, may have associated radial fracturing, often visible only in the SAR images. A flattened interior and an annular moat characterize the 93 circular coronae; portions of their interiors may be lower than the surrounding plains. These typically have concentric fractures and more well-defined lava flows. Calderic coronae, with more than 50% of the interior lower than the surrounding plains, constitute the majority (188), displaying raised rims and annular moats. The appeal of this classification is that the three groups may represent evolutionary stages of coronae development: the domal set being incipient, active features, the circular representing middle stage, and the calderic the terminal stage of coronae development. In addition, we use the entire set of coronae to compare correlation patterns with the component stage groups.

For craters we use the crater data set of Phillips *et al.* (1992) (Phillips and Izenberg, pers. commun. 1994) with 940 craters, of which 158 have been characterized as "tectonized" and 55 as "embayed." Embayed craters experience encroachment by plains volcanism and tectonized craters are altered by faulting; we adopt this set in our analysis because of these additional characterizations.

Chasmata, linear to arcuate troughs with ridges extending thousands of kilometers, show the greatest relief on Venus, as much as 7 km over a horizontal distance of 30 km, and they have been interpreted as rift zones (Solomon *et al.* 1992). Schaber (1982) has defined a series of rift zones on Venus and described them by great circle arcs, using Pioneer-Venus radar data. Although updated by Magellan, the simplicity of the representation is convenient. Following this approach we represent the rift zone system by five great circle arcs, with a total length of about 55,000 km, 50% greater than the planet's circumference. In addition to the representation of the chasmata by 5 arcs, we use the full set of rifts as defined by Price and Suppe (1995). We arbitrarily number these arcs with increasing longitude (Fig. 1). The first arc through Lada Terra extends from (30°S, 0°) to (30°S, 130°), about 11,000 km. The longest of the rift zones, referred to as the Aphrodite–Beta zone extends half-way around Venus, roughly 22,000 km, which we represent by the second and third arcs, from (10°S, 70°) to (25°S, 150°), and then from (25°S, 150°) to (25°N, 280°). The fourth arc, including Themis–Atla, 15,000 km in length, extends from (25°N, 180°) to (40°S, 320°). The fifth arc, Beta-Phoebe extends from (40°N, 285°) to (20°S, 285°), more than 6000 km. The chasmata themselves deviate from these arcs by as much as 10° of angular distance; indeed 20° swaths about these arcs encompass fully 90% of the "rift zones" (Price and Suppe 1995, Tanaka *et al.* 1997). (The arcs are modified from those used by Stefanick and Jurdy (1996) to better fit the full set of rifts.) Using this full set of detailed rifts zones provides a more accurate representation of the entire system; the rifts and numbered great circle arcs are shown in Fig. 1. The coronae groups and rifts are shown in Fig. 2 along with the positive geoid superimposed.

METHOD

Cataloged objects such as corona types or crater types have nonuniform distributions over the planet's surface and many of the types seem to associate with or avoid each other. We would

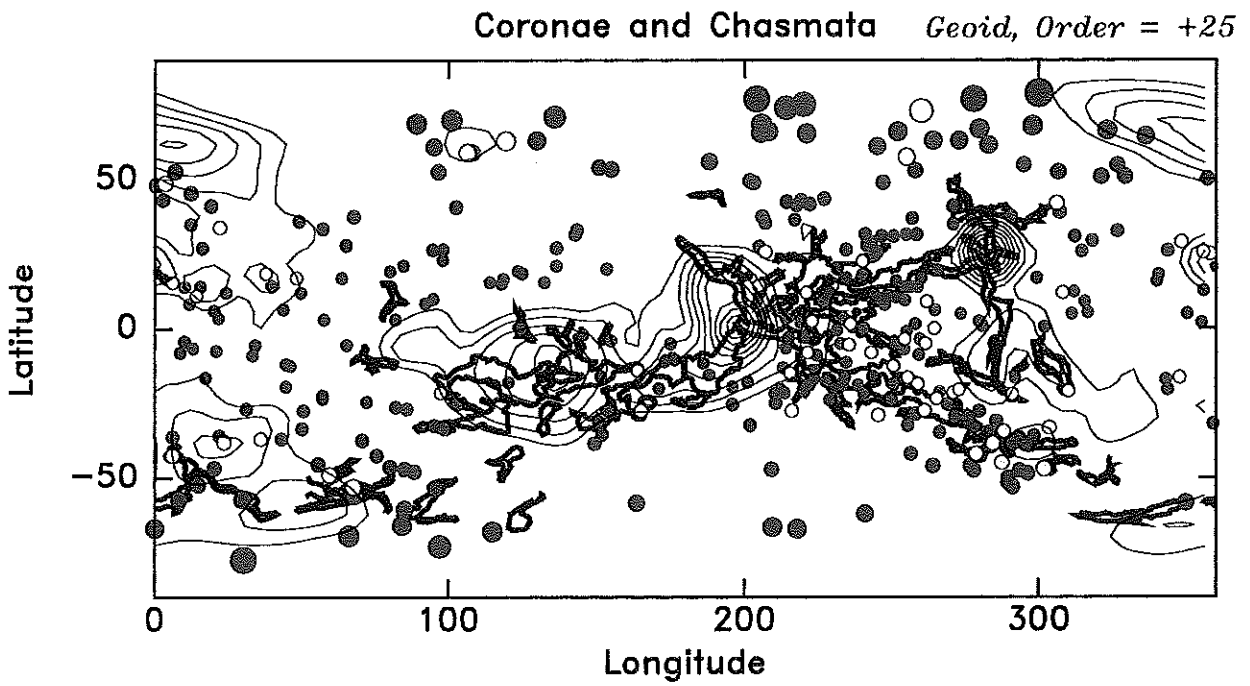

FIG. 2. Distribution of coronae (classification of DeLaughter and Jurdy (1998)), with 50 domal coronae shown as yellow, 93 circular coronae shown as green, and the 188 calderic coronae are shown as blue. Rifts as defined by Price and Suppe (1994) are shown in magenta. The positive geoid, order 25, is overlain.

obtain a quantitative measure of their association if we could subdivide the surface into equal parts and count the number of parts containing each type. We would then compare the number of parts that contain both types, with what would be expected if their distributions were independent. A 2×2 contingency table is used to test whether the associations are statistically significant. In the Appendix a specific example is discussed: comparison of the distribution of coronae with that of rifts and assessment of the significance of association.

The surface of a sphere can be divided into 20 equal equilateral triangles, a dodecahedron, and then each triangle subdivided into 4 nearly equal triangles by bisecting each edge, giving 80, 320, 1280 triangles, etc. The bookkeeping is daunting, and the triangles are not exactly equal anyway. Instead we have taken an indirect approach using an ordinary latitude–longitude grid. For each type of object we define a function $\rho(\bar{r})$ so that if the object type occurs within a certain angular distance θ_0 to the point $\bar{r}$ the function has a value of 1 or 0. This type of function is usually called a characteristic function for which we use ρ because it is a density.

Then the number of parts, N_1, having the type would be given by the integral

$$N_1 = \frac{N}{A} \int \rho_1 \, dA, \tag{1}$$

and the number of parts containing both types would be given by the integral

$$N_{12} = \frac{N}{A} \int \rho_1 \rho_2 \, dA. \tag{2}$$

Here A is the total surface area, so if the planet radius is one unit, $A = 4\pi$. N is the total number of parts dividing the sphere. Initially a test distance, θ_0, of 3° was chosen because a disk of radius 3° nearly contains a square of side 4°, and a $4° \times 4°$ grid was being used. Each test disk has an area πr^2 so the number N of disks which would cover the sphere's surface area is about $4\pi/\pi r^2 \approx 1444$. Any attempt to cover a sphere with disks always has overlap and gap problems, so this is only an approximation for N. Using this value for N we found that the coronae counts calculated using Eq. (1) were all too large but nearly proportional to the known counts. In the final version a test distance of θ_0 of 4° (rather than 3°) was used. For $\theta_0 = 4°$ using $N = 1350$ gave reasonable counts, i.e., within expected error $\pm\sqrt{N_1}$ for a count N_1. [The full set of 331 coronae covers 0.271 of the planet's surface, corresponding to $N = 1220$, whereas 940 craters cover an area of 0.676 and $N = 1390$, where N is the total number of objects that would occur if the distribution were uniformly random. Of the craters, 158 tectonized ones cover 0.112 of the surface, so $N = 1405$; the 55 embayed ones cover 0.041, with $N = 1218$.]

Figure 3 illustrates this approach geometrically, comparing the distributions of coronae and rifts. The left-slanted area represents those points where the characteristic function for the

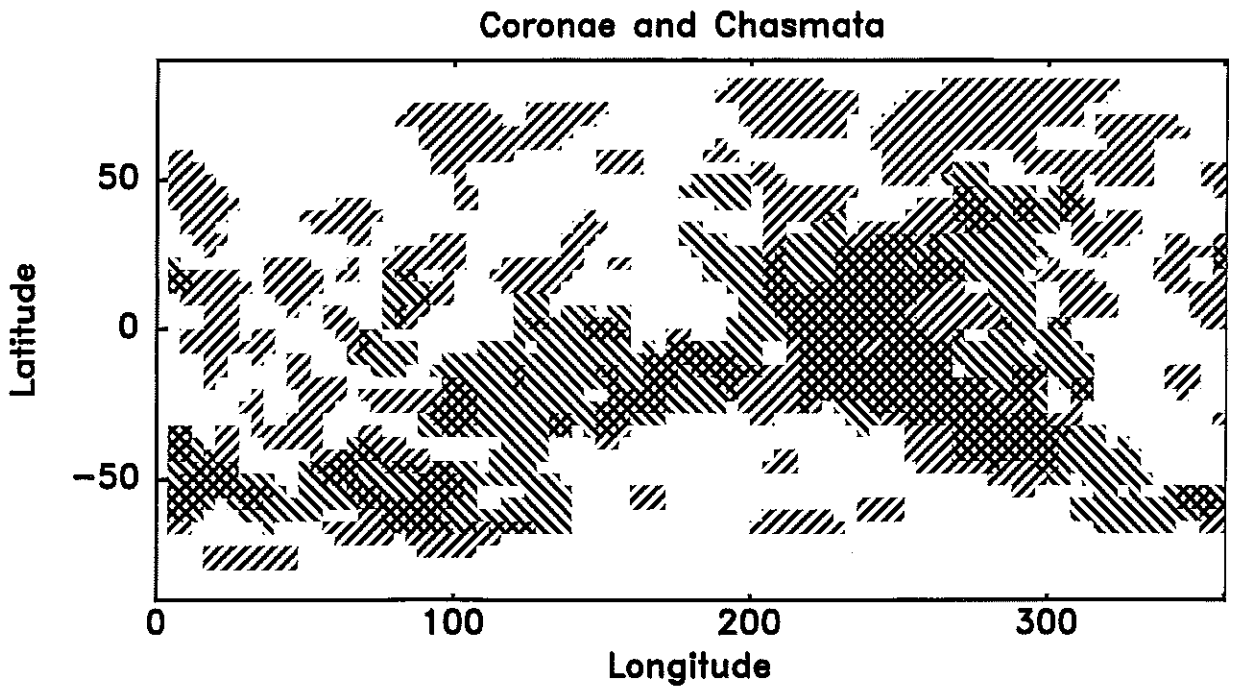

FIG. 3. Characteristic functions for full set of coronae and rifts shown in Fig. 2. Points with only coronae shaded with right-sloping lines, those with only rifts shaded with left-sloping lines, both right- and left-sloping for points with both coronae and rifts, and white for points with neither.

rifts, ρ_1, has the value 1. The right-slanted area similarly represents those points where the characteristic function for the coronae, ρ_2, has the value 1. The region with crossing lines corresponds to the points where both are 1, i.e., the intersection of the two area sets. The white region corresponds to points with neither rifts nor coronae. In constructing the ρ functions described above, the coronae and craters are treated as points at their centers. Counts were made on a latitude–longitude grid with circular search regions of 4°. The rift zones represented by arcs are replaced by a sequence of closely spaced points at about 1°, and these are tested as described above. As can be seen in Fig. 3 the intersected area of coronae and rifts exceeds that expected from chance. The contingency table analysis quantifies the comparison; this example is discussed in detail in the Appendix.

RESULTS

Chasmata, coronae, craters, and subsets are correlated against each other, and the results given in Table I. In this table the χ^2

TABLE I
Correlations between Pairs: Chasmata, Coronae, and Craters

	Chasm	A 1	A 2	A 3	A 4	A 5	Coronae	Domal	Circular	Calderic	Tectonized
Arc 1	99										
Arc 2	99	99									
Arc 3	99	−95	99								
Arc 4	99	−95	−95	99							
Arc 5	99	−90	−90	99	−95						
All Coronae	99	—	−95	99	99	−90					
Domal coronae	99	80	—	—	99	—	99				
Circular coronae	90	90	−80	95	—	−80	99	80			
Calderic coronae	99	−80	—	99	99	−95	99	99	99		
Tectonized craters	99	99	99	99	80	95	−80	—	—	—	
Embayed craters	80	−80	−95	—	95	95	—	—	−80	—	99

Note. Association or avoidance of chasmata, first given as full set of rifts and then by great circle arcs shown in Fig. 1. Coronae are given as full set and then domal group, circular, and calderic. Craters are tectonized and embayed. Values given are probabilities of association, either positive or negative, for 99, 90, and 80%; lesser values are shown as —.

TABLE II
Correlations with Geoid of Chasmata, Coronae, and Craters

	Chasm	A 1	A 2	A 3	A 4	A 5	Coronae	Domal	Circular	Calderic	Tectonized
+	99	99	99	99	99	99	−90	95	—	−99	99
0	−90	−99	−99	−99	99	−99	99	95	—	99	−99
−	−99	−80	−99	−99	−99	−99	−99	−99	—	−80	−99

Note. Correlation is given in percentages for 99th, 90th, and 80th percentiles, less than 80% as —. Geoid arbitrarily divided into thirds by value: +, top third; 0, middle third; −, bottom third. Chasmata, arcs, coronae, and tectonized craters as in Table I.

values have been converted to the probability of the correlation of two occurrences, showing 99, 90, and 80% levels. The form of the table is one common to mileage charts, because of the symmetry of the matrix. Not surprisingly, arcs 1–5 strongly correlate with the full rift set, an agreement apparent in Fig. 1. Similarly, the full coronae set correlates with the full chasmata set, coming from the strong correlation with rifts 3 and 4. Domal coronae, just 1/6th of the total and early stage, correlate strongly with arc 4 and, to a lesser degree, arc 1. The middle stage circular coronae associate with arcs 3 and 1, whereas the final stage calderic group correlates with arcs 3 and 4, avoiding arcs 5 and 1. These associations and avoidances are also apparent in Fig. 2. Tectonized and embayed craters each correlate with rifts. The tectonized craters correlate with arcs 1–5, and the embayed craters correlate with arc 4. Embayed craters avoid arc 2.

Comparison of coronae, craters, and chasmata with the geoid field of Venus is given in Table II. For analysis the geoid field of order 25 was arbitrarily divided by value into three equal thirds: the top indicated as "+," the middle as "0," and the bottom as "−." Most obvious is the strong association of all five chasmata arcs with geoid highs and avoidance with the lows. Only arc 4 shows a positive correlation with intermediate levels; all the others have a negative one. The domal, the youngest coronae, correlate strongly with geoid highs, avoiding lows, but the others show no such correlation. The calderic coronae, the latest stage, correlate, however, with the middle values and avoid geoid highs. Tectonized and embayed craters concentrate near geoid highs, avoiding lows.

DISCUSSION

Coronae on Venus may be analogs of Earth's hotspots. On Earth current hotspot locations clearly stand out from sites of earlier volcanism because of erosion and the separation caused by plate motions. With limited surface displacement on Venus and minimal erosion, active coronae may be hidden among hundreds of relict features. Earth's hotspots correlate strongly with "residual" geoid highs once the effect of subduction is removed (Crough and Jurdy 1980, Chase 1979), an association used to argue for the deep origin of plumes. To isolate the youngest coronae we adopt the classification scheme of DeLaughter and Jurdy (1998) that used altimetry profiles to breakdown coronae into groups related to evolutionary stage. In this classification the domal group of 50, identified by raised interiors and absence of moats, corresponds to the earliest coronae. Indeed, here the domal set is found to positively correlate with geoid highs, whereas later-stage circular and calderic groups do not. Furthermore, the terminal stage, calderic coronae avoid geoid highs at the 99% confidence level. Thus, it appears that on Venus active coronae are associated with geoid highs.

The youngest coronae on Venus are the only ones that correlate with geoid highs. Unfortunately, a unique physical interpretation of lithospheric or plume structure does not directly follow. Noting the paradox of geoid highs associated with both subduction and hotspots on Earth, Richards *et al.* (1988) conclude from their study of models that a "fairly contrived" combination of properties and size is required to produce a positive geoid with a plume. Nonetheless, the same pattern seems to hold on Venus as on Earth: active upwellings with geoid highs. The domal features were identified because of uplifted interiors without evidence of moat development. This suggests current upwelling. Also, DeLaughter and Jurdy (1998, Table 3) show that this group has a lower density and a higher level of tectonism of impact craters than expected, further evidence of current activity. From this we argue that on Venus geoid highs occur with currently active coronae, the domal group, likely locations of rising plumes.

For analysis we use the full set of rifts as well as the representation by five great circle arcs. Areas of extension as defined by Price and Suppe (1995) are fit at the 89.6% level by five arcs, with a total length about of 54,464 km, a circumference and a half. Once corrected for the smaller radius of Venus, this length of extension is within 2.7% of the 59,200 of active spreading ridges estimated for Earth (Parsons 1981). All of the great circle arcs that we use to represent chasmata and rifting strongly correlate positively with geoid highs and negatively with the lows. Alternative interpretations have been proposed about the nature of chasmata. For example, Schubert and Sandwell (1995) argue that chasmata, although being sites of rifting in highlands, may undergo subduction in locations far from highlands, such as near the Latona coronae in the Dali-Diana chasmata system. They do, however, allow that other mechanisms could produce chasmata, such as uplift followed by gravitational relaxation. From our analysis, we conclude that the excellent fit of rift zones using only five great circles suggests a global pattern of extension. The extreme geoid highs are positioned at the intersections of these arcs, with "bulls-eyes" at intersections of arcs 1, 2, and 3 (Beta–Aphrodite), 3 and 4 (Themis–Atla), and 4 and 5 (Beta–Phoebe)

(Fig. 2). Schaber (1982) noticed the intersections of these zones, with Beta and Atla Regiones positioned at the crossings. Curiously, there is a complete absence of coronae at the highest geoid levels (Fig. 2).

Generally, rifting is thought to be among the most recent activity on Venus. Based on the stratigraphy of rifting and volcanism in Atla Regio and the relation with craters having dark parabolic features, Basilevsky (1993) concludes that these impacts and the latest stages of rift activity are contemporaneous, at about 50 Ma if these impact features are indeed among the youngest 10% of craters. In their global sequence of tectonic deformation, Head and Basilevsky (1998) find that linear rifting prevailed in the latest stage of events. Our correlation of surface features on Venus has documented differences in the chasmata, finding that coronae and modified crater association depends on the specific chasmata. In particular, arc 4, Themis to Atla, has a unique clustering of coronae (Fig. 2). Stefanick and Jurdy (1996) find the density of coronae near chasmata twice that expected; here we show that the domal and calderic coronae cluster preferentially near the fourth arc, Themis–Atla. Furthermore, Stofan *et al.* (1997) establish that coronae development occurs at about the same time as rifting. If indeed the domal coronae are the earliest stage, then this arc may represent the most recently, and perhaps longest-lived, site of activity.

APPENDIX

The representation of rifts and coronae by characteristic functions is shown in Fig. 3. If N_1 boxes have only rifts and N_2 boxes only coronae, then the degree of association between two sets is measured by using a 2×2 contingency table. Using this notation the 2×2 contingency table would be

N_{12}	$N_1 - N_{12}$	N_1
$N_2 - N_{12}$	$N - N_1 - N_2 + N_{12}$	$N - N_1$
N_2	$N - N_2$	N

There is only one independent entry in the matrix since the others must sum to the corresponding end column or row. The middle entry corresponds to the calculation of nonintersecting entries in a Venn diagram, containing neither N_1 nor N_2 (white areas in Fig. 3).

The simplest way of measuring the independence or lack of independence of rifts and coronae is to use a ratio test, i.e., to compare the first row with the second row as if they were percentages, then ask whether

$$q_1 = \frac{N_{12}}{N_1}$$

and

$$q_2 = \frac{N_2 - N_{12}}{N - N_1} \tag{3}$$

are significantly different fractions if sampled from the same population. Each population has a sampling error which depends on the probability of the result and the sample size. (As a statistical reference, see for example Bulmer (1979), especially Chap. 9, pp. 139–161.)

The probability of the result is estimated from the column fraction, i.e.,

$$p = \frac{N_2}{N}, \tag{4}$$

and is the same for both samples (rows). The sampling errors for the two rows are then

$$\sigma_1 = \frac{\sqrt{p(1-p)}}{N_1}$$

and

$$\sigma_2 = \frac{\sqrt{p(1-p)}}{N - N_1}, \tag{5}$$

and the combined error is

$$\sigma = \sqrt{\sigma_1^2 + \sigma_2^2} = \sqrt{p(1-p)}\sqrt{\frac{1}{N_1^2} + \frac{1}{(N-N_1)^2}}. \tag{6}$$

The difference in the q values divided by this relative error gives a statistic t, where

$$t = \frac{q_1 - q_2}{\sigma}, \tag{7}$$

which describes how large the difference between the ratios q_1 and q_2 is compared to what might be expected from random samples of size N_1 and $N - N_1$, respectively. One obtains the same result by using columns instead of rows. So the entries in the 2×2 table can be combined into the statistic t, which has the standard normal distribution and whose square has the χ^2 distribution with one degree of freedom. This can be recast as a χ^2 test (Bulmer 1979, pp. 154–156).

As a specific example we will compare the distribution of rifts with that of the coronae using 2×2 contingency tables. Of the 1350 elements, 418 are rifts and 932 are not, and 366 are coronae and 984 are not; 149 elements have both. Figure 3 shows the distribution. The contingency table for this is as follows.

	Coronae	No coronae	Total
Rifts	149	269	418
No rifts	217	715	932
Total	366	984	1350

If the rifts and coronae were statistically independent, entries in the table would factor, i.e., correspond to products of probabilities of independent events, and would be approximately as follows.

	Coronae	No coronae	Total
Rifts	113	305	418
No rifts	253	679	932
Total	366	984	1350

So there are 1.32 times as many elements (149) that are both rifts and coronae as would be expected from chance (113). Is this statistically significant? The probabilities of coronae with and without rifts are $149/418 = 36\%$ and $217/932 = 23\%$. The overall probability, p, of embayed craters is $366/1350 = 27.1\%$, which has a 44% standard deviation; i.e.,

$$\sigma = \sqrt{p(1-p)} = 0.444. \tag{8}$$

With two samples of sizes 418 and 932, respectively, the errors in the difference in their means is given by

$$\varepsilon = \sigma\left[\frac{1}{N_1} + \frac{1}{N - N_1}\right]^{1/2} = 0.444\sqrt{0.003} = 0.026. \tag{9}$$

The difference in the means (36–23%) is 13% (0.13); so the difference is 5 (0.13/0.026) standard deviations, using Eq. (7). The standard deviation is related

to a percentage probability in tables (e.g., Bulmer, (1979), p. 232, Table 2), in this case greater than 99%. A corresponding χ^2 value is significant at the 99% level. Thus, the distribution of coronae and regions of rifting are highly correlated, a very unlikely event (hence the entry in Table I). A negative sign in the table indicates a negative relation; i.e., one type tends to avoid the other type.

ACKNOWLEDGMENTS

We thank Eric Grosfils and Robert Herrick for their interest and thoughtful reviews. Maribeth Price was most helpful in providing digitized rift zones and pointed out the absence of coronae at the rifts with the highest geoid. This research was funded by the Venus Data Analysis Program.

REFERENCES

Basilevsky, A. T. 1993. Age of rifting and associated volcanism in Atla Regio, Venus. *Geophys. Res. Lett.* **20**, 883–886.

Bulmer, M. G. 1979. *Principles of Statistics*. Dover, New York, NY.

Chase, C. G. 1979. Subduction, the geoid, and lower mantle convection. *Nature* **282**, 464–468.

Crough, S. T., and D. M. Jurdy 1980. Subducted lithosphere, hotspots, and the geoid. *Earth Planet. Sci. Lett.* **48**, 15–22.

Crumpler, L. S., J. C. Aubele, D. A. Senske, S. T. Keddie, K. Magee, and J. W. Head 1997. Volcanoes and centers of volcanism on Venus. In *Venus II*. (S. W. Boucher, D. M. Hunten, and R. J. Phillips, Eds.), pp. 697–756. Arizona University Press, Tucson.

DeLaughter, J. E., and D. M. Jurdy 1997. Venus resurfacing by coronae: Implications from impact craters. *Geophys. Res. Lett.* **24**, 815–818.

DeLaughter, J. E., and D. M. Jurdy 1999. Corona classification by evolutionary stage. *Icarus* **139**, 81–92.

Head, J. W., and A. T. Basilevsky 1998. Sequence of tectonic deformation in the history of Venus: Evidence from global stratigraphic relationships. *Geology* **26**, 35–38.

Herrick, R. H., and R. J. Phillips 1994. Implications of a global survey of venusian impact craters. *Icarus* **111**, 387–416.

Magee Roberts, K., and J. W. Head 1993. Large-scale volcanism associated with coronae on Venus: Implications for formation and evolution. *Geophys. Res. Lett.* **20**, 1111–1114.

Parsons, B. 1981. The rates of plate creation and consumption. *Geophys. J. R. Astron. Soc.* **67**, 437–448.

Phillips, R. J., R. F. Raubertas, R. E. Arvidson, I. C. Sarkar, R. R. Herrick, N. Izenberg, and R. E. Grimm 1992. Impact craters and Venus resurfacing history. *J. Geophys. Res.* **97**, 15923–15948.

Price, M., and J. Suppe 1995. Constraints on the resurfacing history of Venus from the hypsometry and distribution of tectonism, volcanism, and impact craters. *Earth Moon Planets* **71**, 99–145.

Richards, M. A., B. H. Hager, and N. H. Sleep 1988. Dynamically supported geoid highs over hotspots: Observations and theory. *J. Geophys. Res.* **93**, 7690–7708.

Schaber, G. G. 1982. Venus: Limited extension and volcanism along zones of lithospheric weakness. *Geophys. Res. Lett.* **9**, 499–502.

Schubert, G., and D. T. Sandwell 1995. A global survey of possible subduction sites on Venus. *Icarus* **117**, 173–196.

Solomon, S. C., S. E. Smrekar, D. L. Bindschadler, R. E. Grimm, W. M. Kaula, G. E. McGill, R. J. Phillips, R. S. Saunders, G. Schubert, S. W. Squyres, and E. R. Stofan 1992. Venus tectonics: An overview of Magellan observations. *J. Geophys. Res.* **97**, 13199–13255.

Stefanick, M., and D. M. Jurdy 1996. Venus coronae, craters and chasmata. *J. Geophys. Res.* **101**, 4637–4643.

Stofan, E. R., V. E. Hamilton, D. M. Janes, and S. E. Smrekar 1997. Coronae on Venus: Morphology and origin. In *Venus II* (S. W. Bougher, D. M. Hunten, and R. J. Phillips, Eds.), pp. 931–965. Univ. of Arizona Press, Tucson.

Stofan, E. R., V. L. Sharpton, G. Schubert, G. Baer, D. L. Bindschadler, D. M. Janes, and S. W. Squyres 1992. Global distribution and characteristics of coronae and related features on Venus: Implications for origin and relation to mantle processes. *J. Geophys. Res.* **97**, 13347–13378.

Tanaka, K. L., D. A. Senske, M. Price, and R. L. Kirk 1997. Physiography, geomorphic/geologic mapping and stratigraphy of Venus. In *Venus II* (S. W. Bougher, D. M. Hunten, and R. J. Phillips, Eds.), pp. 667–694. Univ. of Arizona Press, Tucson.